

Segmentation and Classification of Diabetic Retinopathy

Javeria Amin

Department of Computer Science, COMSATS University Islamabad, Wah Campus

ABSTRACT

Due to the severity of diabetes, diabetic retinopathy (DR) is caused. No main indications found in initial phases of DR, but their quantity and severity rise with time. Initial detection of DR over screening may help to stop vision loss. The initial symptoms of DR such as microaneurysms (MAs) hemorrhage (HMs) and exudates (EXs). In this article, a hybrid approach is presented for non-proliferative diabetic retinopathy (NPDR) detection. The suggested method consists of four steps. In the first step contrast enhancement technique is employed and the second step is using variance-based and mean methods for separating background image. The third step is the Global threshold method for the extraction of candidate lesion. Finally, features are extracted for classification. Presented methodology is evaluated using publically available databases with different performance measures.

Keywords: Retinal, Blindness, Blood vessels, Diabetic Retinopathy

© 2019 Published by UWJCS

1. INTRODUCTION

Worldwide, diabetes is a very common disease. It serves as the main cause of visual impairment for the people with less than 50 years of age [1]. When glucose or fructose over gathers in blood, small blood vessels start rupturing due to the less supply of oxygen to cells. In these vessels, any blockage leads to severe damage to the eye. As a result, metabolic rate slows down and leads to changes in micro vessels found in the retina which in turn causes DR. It affects greater than eighty percent of the diabetes patients [2]. In the US every year the rate of DR is, increasing by 12 percent. It is a main cause of blindness for people aged 20-64 years [3].

The micro-aneurysms (MAs) are earlier sign of DR. In this stage the patient does not feel anxiety. This disease brings changes in the size of the blood vessel (swelling) as well as new blood vessels grow. It usually segments into two different steps that are proliferative DR and non-proliferative DR. NPDR (non-proliferative diabetic retinopathy) appears when retina vessels burst, leak white fluid onto its walls and in return causes retina to become wet and swollen. At the following stage there are many symptoms of DR which are to be seen like hemorrhages (HMs), microaneurysms (MAs), hard/ soft exudates (EXs) and also inter-retinal microvascular abnormalities [4]. If these symptoms are detected at the early stage,

then the steps for further treatment can be selected and followed. Fig. 1 shows NPDR lesions.

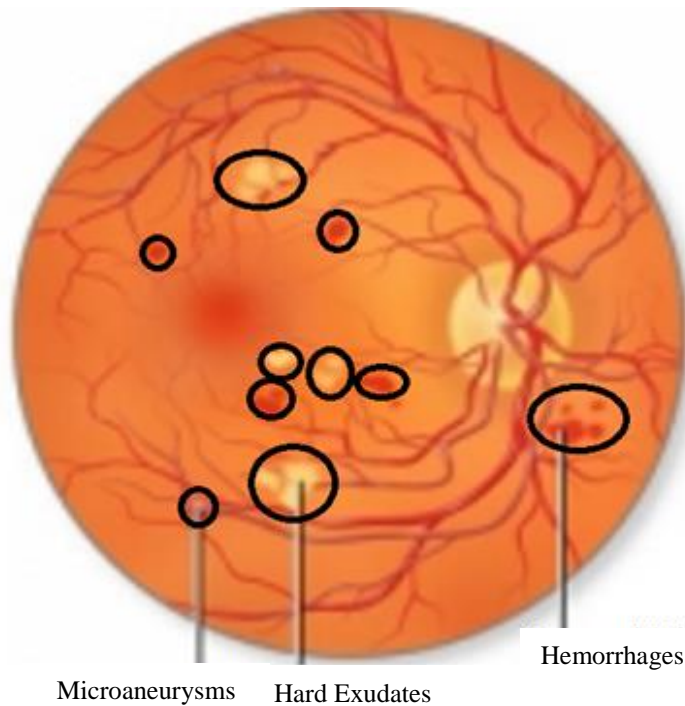


Fig. 1. NPDR Lesions

DR is a dynamic ailment and its identification at an early stage is exceptionally critical for preserving the vision of patient's: this needs regular screening. A computer aided diagnostic system might aid in decreasing the probabilities of the total sightlessness and reduce the workload on ophthalmologists [5].

This paper represents an automatic system in which lesions are present in a retinal image for classification in accordance with several categories of NPDR that are utilized to grade the affected retina.

2. RELATED WORK

DR is a primary reason of visual impairment. There is a great demand for the modern technologies to examine DR appropriately in its initial stage. Recently, many researchers have proposed different image processing techniques for DR detection that are described in this section. For the possibility of increasing the DR screening, many techniques have been

suggested for the detection of lesions such as HMs, EXs and MAs [6],[7]. For the detection of lesion, different techniques can be used such as genetic algorithm [8], dynamic thresholding and multi-scale correlation [9]. AM-FM features extraction and hierarchical clustering methods can also be used for the detection of retinal lesions [10].

3. PROPOSED METHOD

The proposed approach consists of four phases. Lesion region is enhanced using median and histogram equalization method and in second phase different statistical methods are applied for optic disk localization similarly in the third phase global threshold method is applied to segment the DR lesions. The fourth phase extracts different features from each segmented images and performs classification. Algorithm for the major steps of the proposed method is defined below. Fig. 2 shows the overview of the proposed methodology steps graphically.

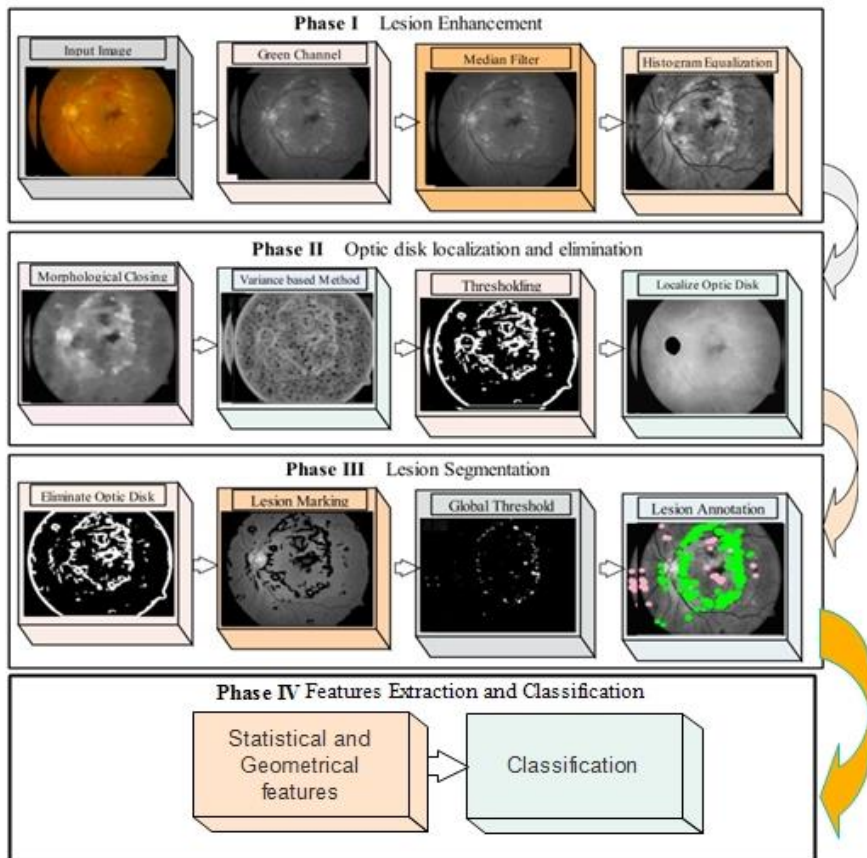


Fig. 2. Overview of the proposed methodology

Algorithm I: Steps of the proposed method for diagnosis of NPDR lesion

- Load datasets
 - Get Green channel
 - Apply median filter
 - Apply local contrast enhancement method
 - Apply local means and variance method
 - Apply global image threshold
 - Extract features for classification
 - Apply classifiers
 - Calculate results
-

A. Image enhancement and segmentation

Automated DR detection from fundus camera is an objective of this research. The purpose of preprocessing is to enhance the region of interest. The green channel from the RGB image of the retinal is further processed using Eq. (1).

$$f_g = \frac{G}{R + G + B} \quad (1)$$

In the next step, median filter of size 3×3 is applied on the processed green channel image to obtain image smoothing f_s . In order to improve the contrast of input image, local histogram equalization is applied to obtain f_c . Images with enhanced contrast are shown in Fig. 3.

During preprocessing, variance and mean based methods are used for separating background image as shown in Eq. (2). Let N denote total number of pixels in a window W of size $m \times n$ and mean_W is the mean of pixel inside W. Window size 7×7 is used.

$$f_{var} = \frac{1}{N - 1} \sum_{i,j \in W} (f_c(i, j) - \text{mean}_W)^2 \quad (2)$$

In the initial stage the image we attained comprises of candidate retinal lesion. Few of them might be false detected. To filter the optic disk (OD) in Eq. (3), total number of pixel in a region called area and boundary pixel known as perimeter.

$$M = 4\pi \frac{\text{area}}{\text{perimeter}^2} \quad (3)$$

A global thresholding is applied for the split-up of OD using T threshold.

$$g(x, y) = \begin{cases} 1 & \text{if } f_{var}(x, y) \leq T \\ 0 & \text{otherwise} \end{cases} \quad (4)$$

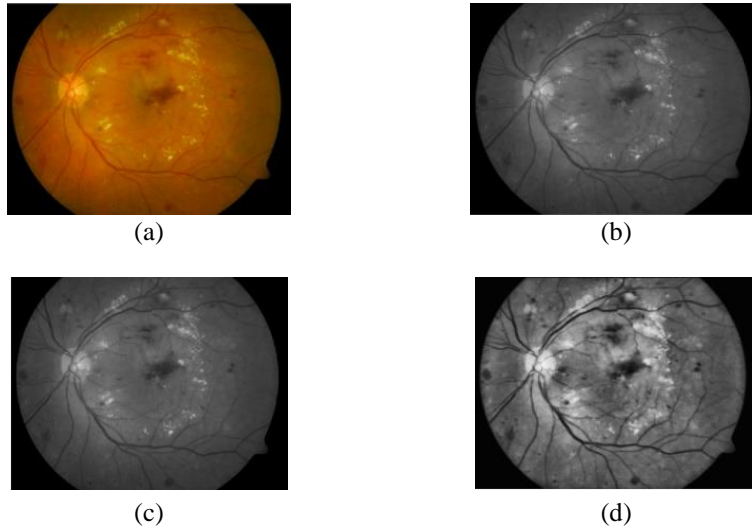


Fig. 3. (a) Original image (b) Green channel (c) Filtered image (d) Image after applying histogram

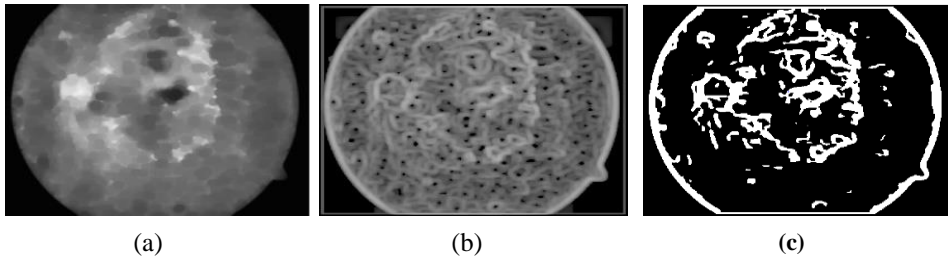


Fig. 4. Segmentation results (a) morphological closing (b) variance based method(c) segmentation

Then, to remove the OD, we applied subtraction operation in described in Eq. (5).

$$g'(x,y) = g(x,y) - f_g(x,y) \quad (5)$$

$$g_m(x,y) = g'(x,y) \oplus se \quad (6)$$

Afterwards, OD is removed by creating marker image through morphological dilation operation as shown in Eq. (6) using disk shape structuring element se . \oplus shows dilation operation. The final result (T2) is achieved using in Eq. (7). Fig. 5 shows the results of retinal lesions.

$$T2 = T(f(x,y) - g_m(x,y)) \quad (7)$$

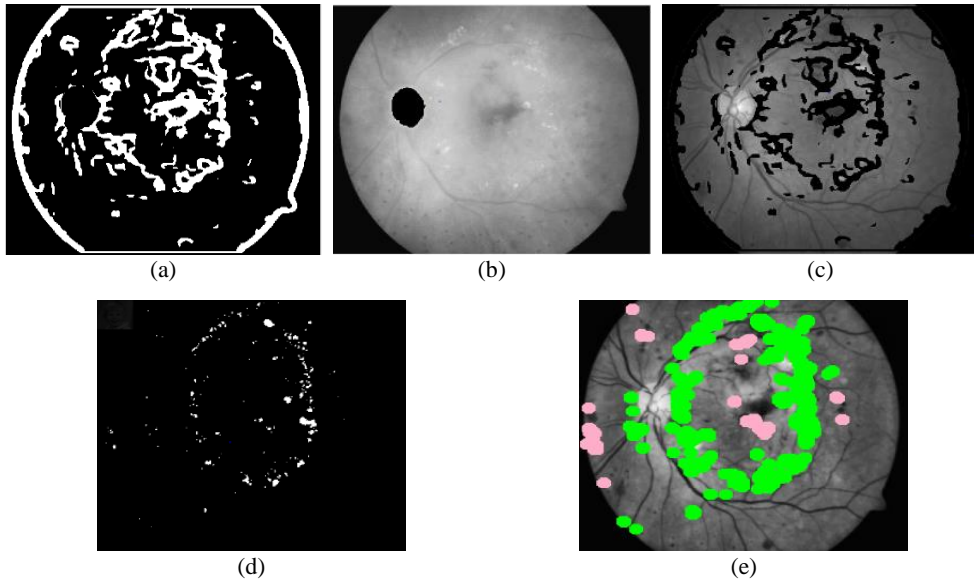


Fig. 5. Results of retinal lesions (a) segment optic disk (b) eliminate optic disk(c) mark the lesion (d) after segmentation (e) annotation of retinal lesion (pink) colour show HMs, MAs and (green) colour show EXs

B. Feature extraction

The retinal lesions appears in different size, shape and color. To differentiate between these lesions for an automated system, four primary features known as: area, radius, circularity, and eccentricity are concatenate/fuse together that is shown in Fig 6. Descriptions of extracted features are described below.

- Area: sum of the total lesion pixels.
- Perimeter: Total number of boundary pixels.
- Circularity : $(4 * \text{Area} * \pi) / (\text{Perimeter} . ^2)$.
- Eccentricity: $\frac{1}{L1} \sqrt{(L1^2 - L2^2)}$ in which L1&L2 denote major/minor axis.

C. Classification

Three different classifications families known as geometric [20], tree [21], and k nearest neighbor [22] are employed in this work. In geometric family, six SVM with linear SVM, quadratic, third one is fine Gaussian and fourth one is cubic SVM, fifth one is medium Gaussian, sixth one is coarse SVM.

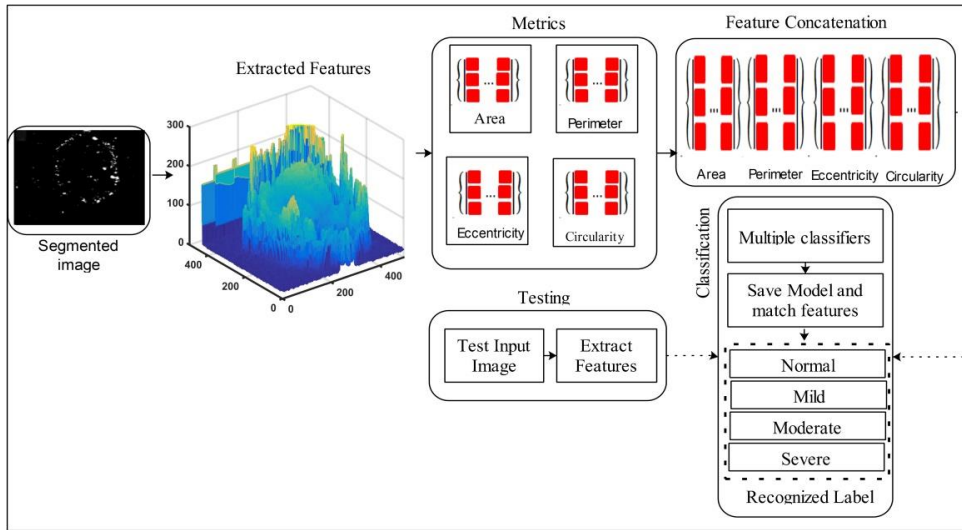


Fig. 6. Proposed feature extraction method

In tree base family we choose Ensemble boosted tree, Ensemble bagged trees, Tree simple, Tree complex, Tree complex classifiers. We have tested five k nearest neighbor classifier, KNN fine, KNN Medium, Cosine, Cubic, and weighted KNN. Comparison of the different classifiers tested based on area under curve (AUC) with 0.5 Hold out validation.

D. Grading of NPDR

In classification, step count the lesions extracted from the retinal images and assign label on the retinal images on the basis of different grades.

- Normal: 0 (healthy images)
- Mild: $0 < MAs \leq 5$
- Moderate: $5 < MAs \leq 15$ and $0 < HMs; EXs \leq 5$
- Severe: Greater quantity of HMs, MAs, and EXs.

Fig. 6 shows grading of NPDR.

4. EXPERIMENTAL RESULTS

In the previous section, performance evaluation of the DR detection method has been defined; five widely presented datasets are used. The Diaretdb1 dataset include 89 images These images are acquired from digital fundus camera and are seen by the angle of 50

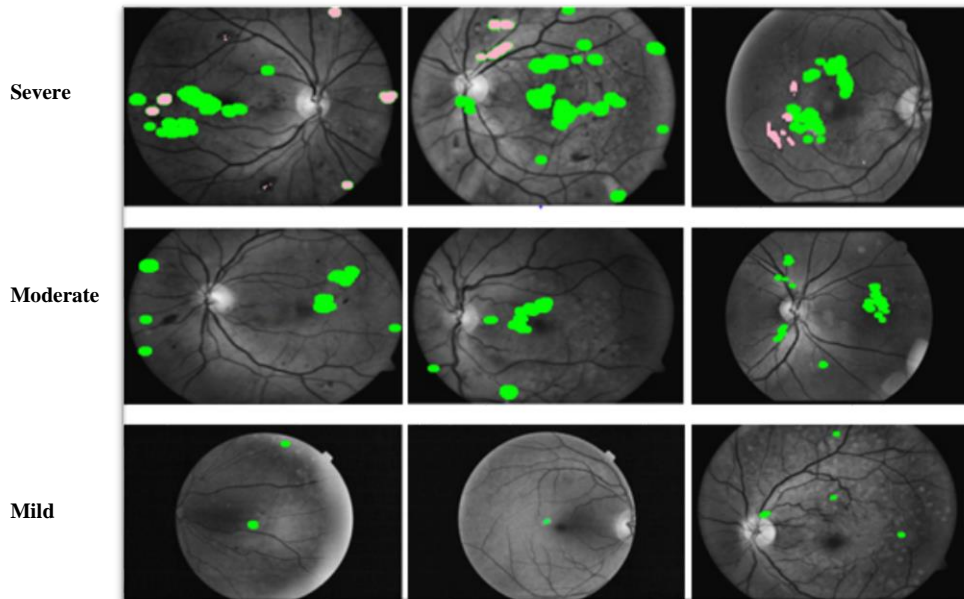


Fig. 7. NPDR Grading

degree[11]. MESSIDOR dataset consists of 1200 eye fundus color images [12]. E-OPHTHA dataset is utilized for the technical study of DR [13]. The VDIS comprised of over 08 images[13]. Local dataset consists of 15 images 9 images are unhealthy and 6 images are healthy.

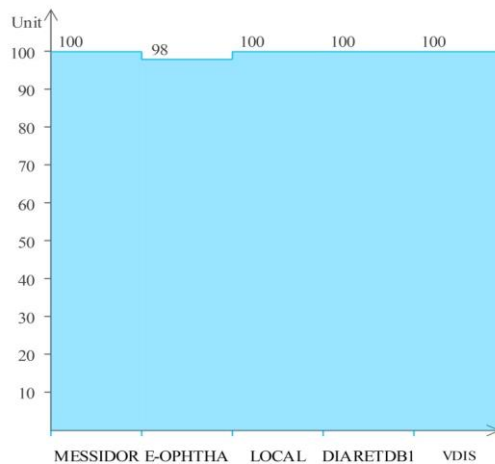


Fig. 8. AUC across each benchmark dataset

The presented system is tested via using five different publically available datasets. We represented the outcomes in under the (AUC) curves and accuracy. The positive images depict symptoms of retinal lesions whereas negative images cannot display any form of disease..

Results of different classifiers are described in Table 1. A comparison result for DR detection is mentioned in Table 2. Maximum accuracy in DIARETDB1 is 95.5% as compared to 100% on the local, VDIS and 97% accuracy on the E-OPHTHA dataset. Graphical representation of AUC on different datasets is shown in Fig. 7.

Table 1. Comparison of different classifiers on different datasets in terms of AUC and Accuracy (lesion level)

Classifier	MESSIDOR Dataset		DIARETDB1 Dataset		E-OPHTHA Dataset		Local Dataset		VDIS Dataset	
	AUC	Acc.	AUC	Acc.	AUC	Acc.	AUC	Acc.	AUC	Acc.
Svm (linear)	0.84	73%	1.00	95.5%	0.82	94%	.81	80%	1.00	100%
Svm (quadratic)	0.86	77%	0.94	90.0%	0.77	90%	.91	80%	1.00	100%
Svm (cubic)	0.96	87%	1.00	95.5%	0.97	95%	.94	80%	1.00	100%
Svm (Gaussian)	0.99	93%	1.00	95.5%	0.73	92%	0.99	96.7%	1.00	100%
Svm (Gaussian medium)	0.87	75%	1.00	86.4%	0.98	93%	.88	76.7%	1.00	100%
Svm (coarse)	67%	0.84%	1.00	63.6%	0.85	97%	.82	70%	1.00	50%
Ensemble (boosted tree)	.83	75%	1.00	90.0%	0.75	89%	1.00	100%	1.00	100%
Ensemble (bagged tree)	1.00	100%	1.00	95.5%	0.68	82%	1.00	100%	1.00	100%
Tree (simple)	.87	75%	1.00	95.5%	0.74	96%	.97	90%	0.50	50%
Tree (medium)	.97	89%	1.00	95.5%	0.79	96%	.97	90%	0.50	50%
Tree (complex)	.97	89%	1.00	95.5%	0.80	96%	.97	90%	0.50	50%
KNN (Fine)	1.00	100%	1.00	95.5%	0.5	91%	1.00	100%	1.00	100%
KNN (Medium)	.83	70%	1.00	95.5%	0.89	85%	.75	73.3%	0.50	50%
KNN (cosine)	.85	72%	1.00	95.5%	0.90	79%	.82	70%	0.50	50%
KNN (cubic)	.85	73%	1.00	95.5%	0.91	97%	.76	70%	0.50	50%
KNN (weighted)	1.00	100%	1.00	95.5%	0.92	91%	1.00	100%	1.00	100%

Table 2. Comparison of the proposed methods with existing methods

Datasets	Methods	Year	Accuracy
DIARETDB1	[4]	2015	95%
	[5]	2014	88%
	[6]	2014	92.96%
	[7]	2018	96.2 %
	Proposed		95.5%
MESSIDOR	[6]	2014	97.5%
	[8]	2018	97.3 %
	Proposed		100%
E-OPHTHA	[9]	2015	92%
	[10]	2018	96.74
	Proposed		97%

5. CONCLUSIONS

In this paper, different grades of the NPDR lesions are segmented and classified. The proposed method accurately remove the optic disk that help to segment the actual lesion region. The hybrid features of segmented images are extracted and supplied to the classifiers. The proposed method obtained 95.5% accuracy on DIARETDB1, 100% accuracy on MESSIDOR and 97% accuracy on E-OPHTHA datasets. The experimental outcomes shows that proposed methodology perform better than existing works.

REFERENCES

- [1] T. Kauppi *et al.*, "The DIARETDB1 Diabetic Retinopathy Database and Evaluation Protocol," in *BMVC*, 2007, pp. 1-10.
- [2] G. J. Chader and E. Y. Chew, "Nutrition and the Environment in Eye Disease," 2007.
- [3] J. H. Kempen *et al.*, "The prevalence of diabetic retinopathy among adults in the United States," *Archives of ophthalmology (Chicago, Ill.: 1960)*, vol. 122, no. 4, pp. 552-563, 2004.
- [4] J. Amin, M. Sharif, M. Yasmin, H. Ali, and S. L. Fernandes, "A method for the detection and classification of diabetic retinopathy using structural predictors of bright lesions," *Journal of Computational Science*, vol. 19, pp. 153-164, 2017.
- [5] H. Narasimha-Iyer *et al.*, "Robust detection and classification of longitudinal changes in color retinal fundus images for monitoring diabetic retinopathy," *IEEE transactions on biomedical engineering*, vol. 53, no. 6, pp. 1084-1098, 2006.
- [6] A. Osareh, M. Mirmehdi, B. Thomas, and R. Markham, "Classification and localisation of diabetic-related eye disease," in *European Conference on Computer Vision*, 2002, pp. 502-516: Springer.
- [7] G. S. Scotland *et al.*, "Costs and consequences of automated algorithms versus manual grading for the detection of referable diabetic retinopathy," *British Journal of Ophthalmology*, vol. 94, no. 6, pp. 712-719, 2010.
- [8] G. Quellec, M. Lamard, P. M. Josselin, G. Cazuguel, B. Cochener, and C. Roux, "Optimal wavelet transform for the detection of microaneurysms in retina photographs," *IEEE Transactions on Medical Imaging*, vol. 27, no. 9, pp. 1230-1241, 2008.
- [9] B. Zhang, X. Wu, J. You, Q. Li, and F. Karray, "Detection of microaneurysms using multi-scale correlation coefficients," *Pattern Recognition*, vol. 43, no. 6, pp. 2237-2248, 2010.
- [10] C. Agurto *et al.*, "Multiscale AM-FM methods for diabetic retinopathy lesion detection," *IEEE transactions on medical imaging*, vol. 29, no. 2, pp. 502-512, 2010.
- [11] M. Christopher, D. C. Moga, S. R. Russell, J. C. Folk, T. Scheetz, and M. D. Abramoff, "Validation of tablet-based evaluation of color fundus images," *Retina*, vol. 32, no. 8, p. 1629, 2012.
- [12] B. Laÿ, "Analyse automatique des images angiofluorographiques au cours de la rétinopathie diabétique," *Ecole Nationale Supérieure des Mines de Paris, Centre de Morphologie Mathématique, France*, 1983.

- [13] C. R. Chand and J. Dheeba, "Automatic detection of exudates in color fundus retinopathy images," *Indian Journal of Science and Technology*, vol. 8, no. 26, 2015.
- [14] D. S. S. Raja and S. Vasuki, "Screening diabetic retinopathy in developing countries using retinal images," *Applied Medical Informatics*, vol. 36, no. 1, p. 13, 2015.
- [15] K. Soman and D. Ravi, "Detection of exudates in human fundus image with a comparative study on methods for the optic disk detection," in *Information Communication and Embedded Systems (ICICES), 2014 International Conference on*, 2014, pp. 1-5: IEEE.
- [16] M. U. Akram, S. Khalid, A. Tariq, S. A. Khan, and F. Azam, "Detection and classification of retinal lesions for grading of diabetic retinopathy," *Computers in biology and medicine*, vol. 45, pp. 161-171, 2014.
- [17] C. Agurto *et al.*, "A multiscale optimization approach to detect exudates in the macula," *IEEE journal of biomedical and health informatics*, vol. 18, no. 4, pp. 1328-1336, 2014.
- [18] G. Quellec *et al.*, "A multiple-instance learning framework for diabetic retinopathy screening," *Medical image analysis*, vol. 16, no. 6, pp. 1228-1240, 2012.
- [19] J. Kaur and D. Mittal, "Segmentation and measurement of exudates in fundus images of the retina for detection of retinal disease," *Journal of Biomedical Engineering and Medical Imaging*, vol. 2, no. 1, p. 27, 2015
- [20] N. Cristianini and J. Shawe-Taylor, *An introduction to support vector machines and other kernel-based learning methods*: Cambridge university press, 2000.
- [21] L. Breiman, J. Friedman, R. Olshen, and C. Stone, "Classification and regression trees–crc press," *Boca Raton, Florida*, 1984.
- [22] L. E. Peterson, "K-nearest neighbor," *Scholarpedia*, vol. 4, p. 1883, 2009.